

Multi-dimensional Photonic Processing, A Discrete-Domain Approach: Part II – Decomposition Techniques and Implementation Using Fiber Optic Delay Lines

Le Nguyen Binh

Department of Electrical and Computer Systems Engineering,
Monash University, Clayton Victoria 3168 Australia.

Abstract

Ultra high bandwidth properties of fiber-optic signal processing systems could provide the necessary processing power for computationally demanding two-dimensional signal processing applications. The techniques of fiber-optic signal processing so far have not been applied to the area of two-dimensional signal processing. Further the matured fields of integrated optics and integrated photonics as well as recent developments of nano-photonics allow innovative structures for processing of lightwaves in photonic domain. This paper as Part II of three part series on multi-dimension photonic signal processing, has sought to integrate the fields of discrete signal processing and fiber-optic signal processing, integrated photonics and/or possibly nano-photonics to establish a methodology based on which physical systems can be implemented. Several photonic signal processing (PSP) architectures are proposed to enable efficient coherent lightwave signal processing. Although the structures are originally developed for 2-D processing, they are also applicable for 1-D structures. Using a combination of one-dimensional filter structures, 2-D fiber-optic filters can be constructed. The relationship between the fiber-optic model and the mathematical model has been linked to allow quick implementation. Using the developed methodologies, multi-dimensional coherent photonic signal processors can be designed.

Key words:

Multi-dimensional, Discrete-Domain, Fiber Optic.

1. Introduction

This paper is the Part II of the series of three parts on multi-dimension photonic signal processing. Part I outlines the motivation of this work and the fundamental theory for multi-dimension signal processing applicable in photonic domain.

The demand for multi-dimensional photonic signal processing (M-D PSP) can be attributed to various factors due the growing feasibility of high-capacity digital transmission networks capable of transmitting ultra-high bit rate and time division multiplexing up to 160 Gb/s as well as fiber optical sensor networks.

A problem with the implementation of such systems is the lack of devices that are capable of processing an enormous

amount of data associated with multi-dimensional signals. With photonic transmission networks becoming the transport infrastructure, PSP technique has become increasingly more desirable compared to O/E and E/O conversion techniques. As discussed in Part I, fiber-optic signal processing systems are ideal for such processing demands for several reasons: all-optical (or photonic) processing of photonic information of optical communication systems are possible using fiber-optic signal processing; 2-D signals usually require much higher bandwidth than 1-D signals and therefore must be processed by a high bandwidth system to allow real-time performance; it is likely that future telecommunication networks would be all fiber-optic.

This paper as the Part II of the series, outlines a number of techniques for multi-dimension signal processing which can be implemented in photonic domain and most importantly they must be simplified so that the optical lightwave paths are minimized and thus minimum losses occur in the photonic processors. This is very critical as lightwaves propagation is involved with the overall transmittance of the photonic circuit [1-5]. Thus if loss is high then optical amplification is required. If this amplification is implemented on the same optical integrated circuit then they would occupy a large area of the circuit. Therefore we propose a number of techniques such as the matrix decomposition methods [6, 7] as described in Section 2. We then present the methods for reduction for the design of 2-D optical filters in Section 3. Finally in Section 4 we present an implementation of 2-D optical filters using fiber optic delay lines. Finally Section 4 gives some concluding remarks.

2. Matrix Decomposition Methods

As the second of the two streams of 2-D filter design methods, matrix decomposition methods are introduced. Matrix decomposition methods result in a set of separable 1-D magnitude responses which can be implemented using any 1-D filter design methods. Using either this approach

or direct approach of Part I [1], a transfer function of the desired 2-D filter can be obtained which can then be implemented by the photonic implementation methods.

2.1 Single-Stage Singular Value Decomposition

In Part I, the application of matrix decomposition to 2-D filter design is briefly introduced. Matrix decomposition is a mathematical procedure where a matrix is split into a sum of products of vectors as

$$\mathbf{H} = \sum_{i=1}^n \lambda_i^{1/2} u_i v_i \quad (1)$$

where λ_i is i^{th} eigenvalue of H and u_i and v_i are the decomposed vectors. An example of matrix decomposition is the well-known LU decomposition which splits a matrix into a lower triangular matrix and an upper triangular matrix. The LU decomposition can be used to express a matrix as sum of products of vectors.

LU decomposition

$$\begin{aligned} \mathbf{A} &= \begin{bmatrix} 1 & 2 & 3 \\ 4 & 5 & 6 \\ 7 & 8 & 9 \end{bmatrix} \\ &= \mathbf{P} \cdot \mathbf{L} \cdot \mathbf{U} = \begin{bmatrix} 0 & 1 & 0 \\ 0 & 0 & 1 \\ 1 & 0 & 0 \end{bmatrix} \begin{bmatrix} 1 & 0 & 0 \\ 0.1429 & 1 & 0 \\ 0.5714 & 0.5000 & 1 \end{bmatrix} \begin{bmatrix} 7 & 8 & 9 \\ 0 & 0.8517 & 1.1743 \\ 0 & 0 & 0 \end{bmatrix} \\ &= \begin{bmatrix} 0.1429 \\ 0.5714 \\ 1 \end{bmatrix} \begin{bmatrix} 7 & 8 & 9 \end{bmatrix} + \begin{bmatrix} 1 \\ 0.5 \\ 0 \end{bmatrix} \begin{bmatrix} 0 & 0.8517 & 1.1743 \end{bmatrix} \\ &= \begin{bmatrix} 1 & 1.1432 & 1.4867 \\ 4 & 4.5712 & 5.2429 \\ 7 & 8 & 9 \end{bmatrix} + \begin{bmatrix} 0 & 0.8517 & 1.1743 \\ 0 & 0.4258 & 0.5871 \\ 0 & 0 & 0 \end{bmatrix} = \begin{bmatrix} 1 & 2 & 3 \\ 4 & 5 & 6 \\ 7 & 8 & 9 \end{bmatrix} \\ \mathbf{A} &= \sum_{i=1, x=1, 2, 3}^3 \mathbf{P} \cdot \mathbf{L}_{xi} \cdot \mathbf{U}_{ix} \quad (2) \end{aligned}$$

A decomposition method particularly suited to 2-D filter design needs is the singular value decomposition (SVD). The SVD reduces a 2-D matrix into two matrices U and V , and a diagonal matrix S of singular values of the original matrix. Singular values are related to the eigenvalues of the matrix and the result has the form

$$\begin{aligned} \mathbf{A} &= \mathbf{U} \cdot \mathbf{S} \cdot \mathbf{B} \\ &= \sum_{i=1, x=1, 2, \dots, N}^N \mathbf{U}_{xi} \mathbf{S}_{ii} \mathbf{B}_{xi} \quad (3) \end{aligned}$$

The unique feature of SVD is that the matrix ‘power’ is distributed to the singular values of the matrix in decreasing order of the position of the singular value in the matrix S starting from the top left corner. Consequently, to approximate the matrix A by the product of just one set of two vectors U_{xi} and B_{xi} , the best approximation will be made by the product of first set of vectors that result from SVD of the matrix. Mathematically, the property can be described as shown in Eq. 5-3. As an example, if we wanted to approximate the matrix $\begin{bmatrix} 1 & 2 \\ 3 & 4 \end{bmatrix}$ by the product of a set of vectors, SVD would be performed on the matrix resulting in $U = \begin{bmatrix} 0.4046 & 0.9145 \\ 0.9145 & -0.4046 \end{bmatrix}$, $V = \begin{bmatrix} 0.5760 & 0.8174 \\ -0.8174 & 0.5760 \end{bmatrix}$, and $S = \begin{bmatrix} 5.4650 & 0 \\ 0 & 0.3660 \end{bmatrix}$. $U_{x1} = [0.4046 \ 0.9145]$, $S_{11} = 5.4650$, and $V_{x1} = [0.5760 \ 0.8174]$ form the first set of vectors. The resulting approximation would then be $U_{x1} S_{11} V_{x1}^T = \begin{bmatrix} 1.2736 & 1.8072 \\ 2.8790 & 4.0853 \end{bmatrix}$. To obtain a better approximation of $\begin{bmatrix} 1 & 2 \\ 3 & 4 \end{bmatrix}$, the product of the second set of vectors could be added.

$$\left\| \mathbf{A} - \sum_{i=1, x=1, 2, \dots, N}^N \mathbf{U}_{xi} \mathbf{S}_{ii} \mathbf{B}_{xi}^T \right\| = \min_{\mathbf{U}_{xi}, \mathbf{S}_{ii}, \mathbf{B}_{xi}} \left\| \mathbf{A} - \sum_{i=1, x=1, 2, \dots, N}^N \hat{\mathbf{U}}_{xi}^T \hat{\mathbf{S}}_{ii} \mathbf{B}_{xi}^T \right\| \quad (4)$$

where $\hat{\mathbf{U}}_{xi}^T$ and \mathbf{B}_{xi} are subsets of \mathbf{U}_{xi} and \mathbf{B}_{xi} , and $\hat{\mathbf{S}}_{ii}$ is the corresponding singular value

In [8], the SVD is used to decompose a 2-D magnitude specification matrix into two 1-D magnitude specification. The result is a design procedure in which a 2-D filter design becomes a set of 1-D filter design. The matrix decomposition methods have several advantages over the direct methods of Part I [1] as follows: (i) The resulting 1-D magnitude specifications can be met by any of the standard algorithms for 1-D filter design such as least-squares method or Parks-McClellan algorithms available in many computer simulation packages; (ii) As long as 1-D filter sections are stable, the overall 2-D filter is also stable. The stability of final 2-D design can therefore be guaranteed easily without the need for heavy mathematical analysis or computationally expensive algorithms involved with 2-D filter designs; (iii) The filter designer is given the flexibility to decide how many sets of 1-D filter sections are included in the system; and (iv) The resulting 2-D filter is parallel in structure and therefore does not introduce unnecessary processing delays.

All 2-D filters designed using matrix decomposition can be described by (5) where $F_i(z_1)$ and $G_i(z_2)$ are 1-D filter sections and K is the number of singular values included in the system.

$$H(z_1, z_2) = \sum_{i=1}^K F_i(z_1) \cdot G_i(z_2) \quad (5)$$

A simple example of 2-D filter design using only one filter section as in [2] is given below. The example chosen is deliberately simple to show the fundamental concepts involved in 2-D filter design using matrix decomposition methods.

A 2-D filter design using SVD with single parallel section

Design Aim: A low-pass filter with normalized cut-off frequency of 0.5 in both dimensions.

Method: Single-stage singular value decomposition

Program used: SVDFIR2-D.M

Result: With single stage, the error of frequency response of the designed filter is 6.663%. Although this is quite low, it may not be acceptable in some cases for which an extension of single-stage singular value decomposition may be employed as shown in Section 2.2.

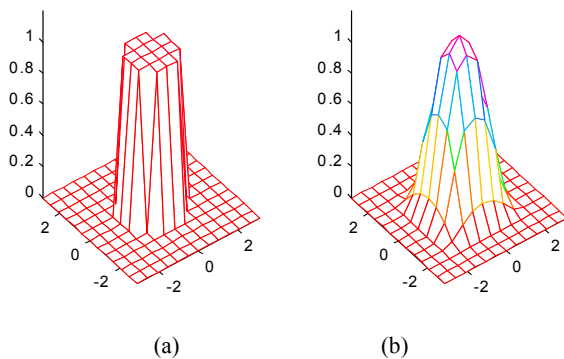


Figure 1:(a) Magnitude specification of low-pass filter (b) Magnitude response of 15×15 2-D filter designed using single stage singular value decomposition

The 1-D filters designed are FIR filters and the actual filter coefficients are given in a table format as shown below. It is noted that the first and the second filter sections are identical since the frequency specification is symmetric about the origin. Consequently for symmetric filters, only one 1-D filter needs to be designed to complete the design for a 2-D filter implying significant simplification in the filter design procedure.

The filter designed in *Table 1*, when implemented takes on the structure shown in *Figure 2*. In case of a multiple-stage implementation, several of the structure shown below would be connected in parallel to form the 2-D filter.

Coefficient order	b_1	b_2
0	-0.0007	-0.0007
1	0.0010	0.0010
2	0.0025	0.0025
3	-0.0090	-0.0090
4	-0.0273	-0.0273
5	0.0197	0.0197
6	0.1837	0.1837
7	0.3553	0.3553
8	0.3553	0.3553
9	0.1837	0.1837
10	0.0197	0.0197
11	-0.0273	-0.0273
12	-0.0090	-0.0090
13	0.0025	0.0025
14	0.0010	0.0010
15	-0.0007	-0.0007

Table 1: Coefficients of the FIR filter designed using single-stage singular value decomposition

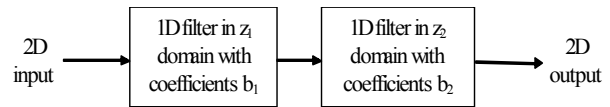


Figure 2: Separable implementation of 2-D filter using single-stage singular value decomposition

2.2 Multiple-Stage Singular Value Decomposition

Multiple-stage SVD takes the leap forward from single-stage SVD method and includes stages that belong to second largest singular values and smaller. Depending on the relative magnitude of singular values, the inclusion of extra stages can result in a sizable reduction in error, or sometimes it has no effect at all. The sampled design given below shows a case where inclusion of multiple stages results in more than 30% reduction in the error of the single stage implementation.

A 2-D filter design using SVD with multiple parallel sections.

Design Aim: A 90° fan filter of order of 32×32

Method: Multiple stage singular value decomposition with 1-D FIR filters

Program used: SVDFIR2-D.m

Result: The error of frequency response of the filter is given as 18.65%¹.

¹ Although this value is quite large compared to the single digit figure we have been obtaining so far, it should be kept in mind that the error largely depends on the specification. Therefore it is only meaningful to compare error between different implementations of the same magnitude specification.

The filter is obtained after six parallel stages. *Figure 4* shows the error and magnitudes of the singular values against the number of included parallel stages. *Figure 4* appears to show that there is roughly a linear relationship between the error curve and the singular values curve. The relationship is actually more subtle than this. A little thought will reveal that greater the gradient of singular value curve is, flatter the error curve will be. This is because if there is a large difference between two singular values, adding the stage which belongs to the smaller singular value will have little effect on the overall performance. As a rule of thumb, if the singular value of a parallel stage is less than one-tenth of the first singular value, then it is probably not worth including.

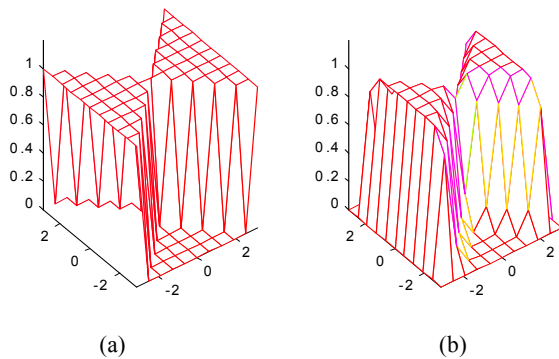


Figure 3(a) Magnitude specification of 90° fan filter (b) Magnitude response of 32x32 2-D filter designed using multiple-stage singular value decomposition.

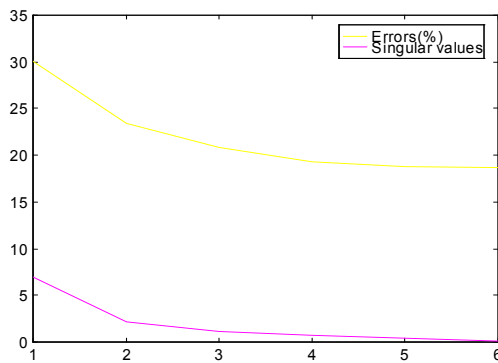


Figure 4: Errors and magnitudes of singular values

With the current computer technology, calculations for around ten 32nd order 1-D filters can be done virtually in real time and therefore the SVD method is practical even for adaptive filtering. The resulting filter structure is shown in *Figure 5*.

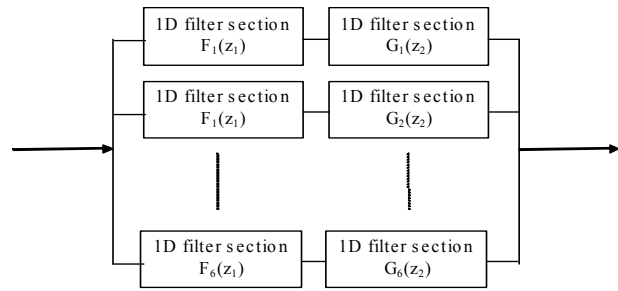


Figure 5: Structure of 2-D 90° fan filter

2.3 Iterative Singular Value Decomposition

There are many variations on the theme of matrix decomposition, in particular the SVD. The iterative singular value decomposition (ISVD)[18] is devised in order to avoid ‘negative’ magnitude definitions that arises from the plain SVD procedure of the previous section. By keeping the 1-D magnitude positive, the paper claims that the 1-D filter design procedure becomes less intricate.

Iterative singular value decomposition [19]

1. Let the 2-D magnitude specification be A . Let $A_1^+ = A$ and $A_1^- = 0$.
2. Perform singular value decomposition on A_1^+ . λ_{1i} are the singular values of A_1^+ . By the definition of SVD given in [18], λ_{11} is larger than any other λ s.

$$\begin{aligned}
 \mathbf{A}_1^+ &= \sum_{i=1}^{r_1} \lambda_{1i} \mathbf{u}_{1i} \mathbf{v}_{1i}^t \\
 &= \sum_{i=1}^{r_1} \mathbf{u}_{1i} \lambda_{1i}^{1/2} \cdot \lambda_{1i}^{1/2} \mathbf{v}_{1i}^t
 \end{aligned}$$

3. Because of Perron’s result on non-negative matrices [18], the vectors \mathbf{u}_{11} and \mathbf{v}_{11} are also non-negative. It is then possible to estimate A^+ by $\mathbf{u}_{11} \lambda_{11}^{1/2} \cdot \lambda_{11}^{1/2} \mathbf{v}_{11}^t$. Assigning the first of the pair as F_1^+ and G_1^+ gives the first non-negative 1-D magnitude specifications. F_1 and G_1 are assigned F_1^+ and G_1^+

$$\begin{aligned}
 S_1 &= 1 \\
 \mathbf{F}_1 &= \mathbf{F}_1^+ \\
 \mathbf{G}_1 &= \mathbf{G}_1^+
 \end{aligned}$$

4. A_2 can now be calculated using *Eq. 5-5*. This matrix can now be separated into \mathbf{A}_2^+ and \mathbf{A}_2^- sum of which make up the error matrix A_2 .

$$\begin{aligned} \mathbf{A}_2 &= \mathbf{A} - S_1 \mathbf{F}_1 \mathbf{G}_1 \\ &= \mathbf{A}_2^+ + \mathbf{A}_2^- \end{aligned} \tag{6}$$

where

$$\begin{aligned} A_2^+(m,n) &= A_2(m,n) && \text{if } A_2(m,n) \geq 0 \\ &= 0 && \text{if } A_2(m,n) < 0 \\ A_2^-(m,n) &= A_2(m,n) && \text{if } A_2(m,n) < 0 \\ &= 0 && \text{if } A_2(m,n) \geq 0 \end{aligned}$$

5. Singular value decomposition is performed on both matrices resulting in two sets of vectors $S_2, \mathbf{F}_2^+, \mathbf{G}_2^+$ and $S_2, \mathbf{F}_2^-, \mathbf{G}_2^-$. S_2 is 1 for the vectors resulting from decomposition of \mathbf{A}^+ , and -1 for the vectors from \mathbf{A}^- .

6. Euclidean norms are calculated for resulting error matrix defined in Eq. 5-6. The same operation is performed with $S_2, \mathbf{F}_2^-, \mathbf{G}_2^-$ in place of $S_2, \mathbf{F}_2^+, \mathbf{G}_2^+$ in Eq. 5-6 with E_2^- as the result.

$$\begin{aligned} \mathbf{E}_2^+ &= \mathbf{A} - \sum_{i=1}^2 S_i \mathbf{F}_i^+ \mathbf{G}_i^+ \\ \|\mathbf{E}_2^+\|_2 &= \left\{ \sum_{m=0}^M \sum_{n=0}^N [E_2^+(m,n)]^2 \right\}^{1/2} \end{aligned} \tag{7}$$

7. E_2^+ and E_2^- are compared. Since smaller error means closer approximation to the original matrix, the set of vectors that results in the lower Euclidean norm is chosen as \mathbf{F}_2 and \mathbf{G}_2 .

8. \mathbf{A}_3 is assigned the error matrix $\mathbf{A}_2 - \mathbf{A}^+$ or $\mathbf{A}_2 - \mathbf{A}^-$ depending on whether E_2^+ is greater or smaller than E_2^- . Steps 4,5,6 and 7 are then repeated with appropriate substitution. The procedure is repeated until a satisfactory approximation of the original matrix is obtained.

Compared to plain singular value decomposition algorithm, ISVD algorithm converges more slowly because adding an extra stage does less to compensate for the error than plain SVD algorithm since only a part of the error is compensated. An example of a filter designed using the iterative singular-value decomposition is given as

2-D Filter design example using iterative singular value decomposition

Design aim: A bandpass filter of order of 32x32 with normalized passband between 0.3 and 0.6.
 Method: Iterative singular value decomposition algorithm
 Program used: ISVDFIR2-D.m
 Result:

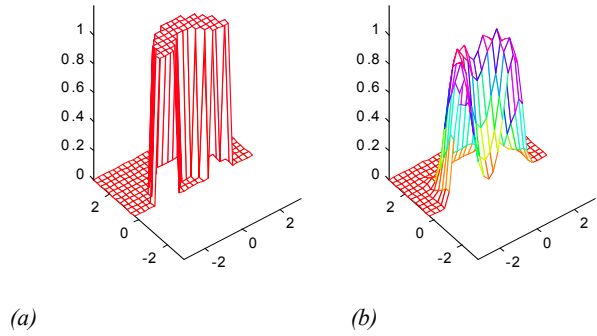


Figure 6: Iterative singular value decomposition (a) Ideal magnitude response (b) Actual filter magnitude response

The filter error is reasonably low at 9.88% after seven approximation stages. Overall, the filter requires seven 1-D FIR filter design stages as the magnitude specification is symmetric about the two axis. Because of the complexity of the magnitude specification, the designed filter does not perform as well as one might expect. This can be corrected to some extent using better 1-D filter design procedures such as the Parks-McClellan algorithm.

2.4 Optimal Decomposition

Optimal decomposition is an improvement on ISVD which is based on optimization of the 1-D magnitude vectors so that the Euclidean error is minimized. The error is found to be 9.68%, which is only slightly better than that of ISVD.

Optimal decomposition[4]

In Eq. 5-6, the definition of the Euclidean norm is defined. In the optimal decomposition, the objective is to minimize the value of this error estimate to provide the best set of vectors that will make up the original specification matrix. Continuing with the constraint that magnitude vectors must all be positive, we then perform exponential mapping to \mathbf{F}_i and \mathbf{G}_i .

$$\begin{aligned} \mathbf{F}_i &= [e^{x_{i0}} \quad e^{x_{i1}} \quad \dots \quad e^{x_{iM}}] \\ \mathbf{G}_i &= [e^{y_{i0}} \quad e^{y_{i1}} \quad \dots \quad e^{y_{iN}}] \end{aligned} \tag{8}$$

The purpose of exponential transformation is so that the optimizing variables x_{ij} and y_{ij} are not constrained to be positive. However the condition of positive magnitude is retained as all values of \mathbf{F}_i and \mathbf{G}_i will be positive no matter what the values of x_{ij} and y_{ij} are. Non-linear optimizing technique must be applied since this problem is non-linear. Numerous algorithms exist for non-linear optimization of several variables and any technique can be used to obtain the answer.

Choosing bad starting points for optimization routines results in local minima or bad convergence points and it recommended that iterative singular value decomposition algorithm be used to provide the initial points for optimization.

2-D filter design example using optimal decomposition

Design aim: A 2-D bandpass filter with normalized passband frequencies of 0.33 and 0.66 in both dimensions.

Method: Optimal decomposition[6]

Program used: ODFIR2-D.m

Result: The error is 9.65% compared to 9.88% for ISVD algorithm after seven stages. The number of filter designs required is seven(same as ISVD), however each filter stage requires a great deal more computational effort than the ISVD method as it requires non-linear optimization to be performed on quite a large number of variables.

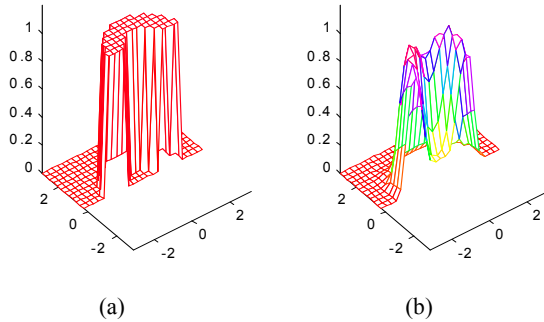


Figure 7: Optimal decomposition(a) Ideal magnitude response(b) Actual filter magnitude response

Due to the computational constraints, full optimization is not performed. Even then the optimization routine took a very long time to perform and the reason is attributed to the number of variables to be optimized being so large (20 to 30 variables depending on the order of the filter transfer function).

2.5 Other 2-D Filter Design Methods Based on Matrix Decomposition

There are many other 2-D filter design methods that are based on the idea of matrix decomposition. So far, all the methods discussed decompose the 2-D magnitude specification into a set of two 1-D magnitude specifications so that the 2-D filter design procedure is essentially reduced to that of 1-D. It is shown that using this approach, the design problem is reduced significantly, but it is also shown that since the approach produces only an approximation to the 2-D transfer function the methods based on magnitude decomposition does not perform as well as direct methods.

One notable 2-D filter design method uses matrix decomposition but is not based on magnitude decomposition is by Shaw and Mistra [7]. In this approach, it is assumed that the 2-D transfer function is already obtained using some 2-D filter design.

A 2-D transfer function can be represented by matrices as shown in (9).

$$H(z_1, z_2) = \frac{h_b(z_1, z_2)}{h_a(z_1, z_2)}$$

$$= \frac{\mathbf{z}_{b1}^T \begin{bmatrix} h_b(n_{b1}-1, m_{b1}-1) & h_b(n_{b1}-1, m_{b1}-2) & \dots & h_b(n_{b1}-1, 0) \\ \vdots & \vdots & \ddots & \vdots \\ h_b(1, m_{b1}-1) & h_b(1, m_{b1}-2) & \dots & h_b(1, 0) \\ h_b(0, m_{b1}-1) & h_b(0, m_{b1}-2) & \dots & h_b(0, 0) \end{bmatrix} \mathbf{z}_{b2}}{\mathbf{z}_{a1}^T \begin{bmatrix} h_a(n_{a1}-1, m_{a1}-1) & h_a(n_{a1}-1, m_{a1}-2) & \dots & h_a(n_{a1}-1, 0) \\ \vdots & \vdots & \ddots & \vdots \\ h_a(1, m_{a1}-1) & h_a(1, m_{a1}-2) & \dots & h_a(1, 0) \\ h_a(0, m_{a1}-1) & h_a(0, m_{a1}-2) & \dots & h_a(0, 0) \end{bmatrix} \mathbf{z}_{a2}}$$

where

$$\mathbf{z}_{b1} \triangleq [z_1^{bm_1-1} \ z_1^{bm_1-2} \ \dots \ z_1 \ 1]^T$$

$$\mathbf{z}_{b2} \triangleq [z_2^{bm_2-1} \ z_2^{bm_2-2} \ \dots \ z_2 \ 1]^T$$

$$\mathbf{z}_{a1} \triangleq [z_1^{am_1-1} \ z_1^{am_1-2} \ \dots \ z_1 \ 1]^T$$

$$\mathbf{z}_{a2} \triangleq [z_2^{am_2-1} \ z_2^{am_2-2} \ \dots \ z_2 \ 1]^T$$

(9)

In Shaw's method, the decomposition is performed on 2-D transfer function matrices. The method can result in efficient filters in terms of the required elements, however it results in 1-D filter sections with different orders and thus does not offer the modularity of the other decomposition methods [7]. Other methods exist for yet more efficient filter design and a 2-D filter order reduction method is described in Part I [1].

3. 2-D Filter Order Reduction Using Balanced Approximation Theory

Keeping the filter order to the minimum is important for photonic circuit implementation as coupling losses of higher order filters may render the actual implementation impossible. To achieve lower order filters with good performance, the balanced approximation method used in control systems theory is applied to the order reduction of 2-D digital filters.

3.1 Motivation for Lower Order Photonic Filters

For an adequate filter performance, that is satisfying the roll-off factor and the passband ripple, the order of the filter must be appropriately chosen. In general, increasing the order of the filter can significantly reduce the error.

However, higher filter order directly translates to extra filter components, noise, and higher attenuation which are unacceptable in many cases including fiber-optic implementations. It is therefore critical that the order of the filter remains low without sacrificing overall performance measures such as error response.

The motivation for keeping filter order low is greater for fiber-optic systems than in other filter implementations for the reason that higher order filters cause large coupling loss which must be compensated by a pre-amplifier which in turn introduces noise when the amplification factor is large. It is generally accepted that filters with order greater than 16 start becoming difficult to realize in practice with the current technology. However, as we have seen in Sections 2 and 3, 2-D filters with orders of around 30×30 are quite common.

Balanced approximation, derived from control theory, is a model reduction technique for 1-D systems. As 2-D filters usually have high orders, application of the filter order reduction method to 2-D filters may prove to be very rewarding especially for fiber-optic filters which must have low orders for feasibility.

3.2 Description of 2-D System in State-Space Format

As balanced approximation is originally developed for model reduction of dynamic systems, it uses the state-space model of digital systems. The implication is that 2-D systems, which we have been representing using transfer functions must now be represented in state-space format.

The representation of 2-D systems in a state-space format has been a topic for research for a number of years and several models have been proposed [22,23]. It is noted in [12] that the model in [22](see Box 3-2) is most general and the model proposed in [23] can actually be embedded into the model in [22].

Although converting from 2-D transfer function description to 2-D state-space description involves only plug-in formulae, converting from 2-D state-space description to 2-D transfer function is much more involved and a novel algorithm is described in Part I [1]. Using the two algorithms, the balanced approximation method can be applied to 2-D systems.

3.3 Balanced Approximation Method

Using a known 2-D filter transfer function, the balanced approximation method (BAM) finds the *balancing transformation* matrix T which ‘balances’ the system. The order reduction is subsequently performed by removing states that do not contribute substantially to the system behavior.

The first task is to find the generalized reachability and observability Gramians defined as

$$\begin{aligned}
 K &= \frac{1}{(2\pi j)^2} \iint_{|z_1|=1} \iint_{|z_2|=1} f(z_1, z_2) f^*(z_1, z_2) \frac{dz_1}{z_1} \frac{dz_2}{z_2} \\
 W &= \frac{1}{(2\pi j)^2} \iint_{|z_1|=1} \iint_{|z_2|=1} g^*(z_1, z_2) g(z_1, z_2) \frac{dz_1}{z_1} \frac{dz_2}{z_2}
 \end{aligned}
 \tag{10}$$

where

$$\begin{aligned}
 f(z_1, z_2) &= [\mathbf{I}(z_1, z_2) - \mathbf{A}]^{-1} \mathbf{b} \\
 g(z_1, z_2) &= \mathbf{c} [\mathbf{I}(z_1, z_2) - \mathbf{A}]^{-1}
 \end{aligned}$$

Fortunately, the double integrations do not have to be solved directly and can be partially solved (as distinct from partial integration) using the Lyapunov approach. If K_{11} denotes the upper left upper block of K and K_{22} denotes the lower right block of K , then K_{11} and K_{22} can be obtained. The same notations apply to the observability Gramian, W .

$$\begin{aligned}
 K_{11} &= \sum_{i=0}^{N_1-1} \mathbf{A}_1^i \mathbf{P} (\mathbf{A}_1^T)^i & W_{22} &= \sum_{i=0}^{N_2-1} \mathbf{A}_2^i \mathbf{Q} (\mathbf{A}_2^T)^i \\
 \text{where} & & \text{where} & \\
 \mathbf{P} &= \mathbf{H}_b \mathbf{H}_b^T & \mathbf{Q} &= \mathbf{H}_c^T \mathbf{H}_c \\
 \mathbf{H}_b &= \begin{bmatrix} h_{10} & \cdots & h_{1N_2} \\ \vdots & \ddots & \vdots \\ h_{N_1 0} & \cdots & h_{N_1 N_2} \end{bmatrix} & \mathbf{H}_c &= \begin{bmatrix} h_{01} & \cdots & h_{0N_2} \\ \vdots & \ddots & \vdots \\ h_{N_1 1} & \cdots & h_{N_1 N_2} \end{bmatrix} \\
 W_{11} &= \mathbf{I}_{N_1} & K_{22} &= \mathbf{I}_{N_2}
 \end{aligned}
 \tag{11}$$

A system is said to be balanced if its Gramians satisfy the following condition where σ_{ij} are the Hankel singular value of the system.

$$\begin{aligned}
 K_{11} = W_{11} &= \begin{bmatrix} \sigma_{11} & 0 & \cdots & 0 \\ 0 & \sigma_{12} & \ddots & \vdots \\ \vdots & \ddots & \ddots & 0 \\ 0 & \cdots & 0 & \sigma_{1N_1} \end{bmatrix} \\
 K_{22} = W_{22} &= \begin{bmatrix} \sigma_{21} & 0 & \cdots & 0 \\ 0 & \sigma_{22} & \ddots & \vdots \\ \vdots & \ddots & \ddots & 0 \\ 0 & \cdots & 0 & \sigma_{2N_2} \end{bmatrix}
 \end{aligned}
 \tag{12}$$

To balance a system, the similarity transform T that will achieve the above condition must be found. Applying the balancing similarity transform T to the subsections of Gramians will result in the condition satisfied.

$$\begin{aligned}
 \hat{K} &= T^{-1} K T^{-T} \\
 \hat{W} &= T^T W T
 \end{aligned}
 \tag{13}$$

The balancing transformation T can be found by applying the algorithm given in [24].

Determination of the balancing transformation T

1. Cholesky factorization of K_{11} : The resulting lower triangular matrix is assigned L_c .
2. Formation of $L_c^T W_{11} L_c$
3. Symmetric eigenvalue/eigenvector problem, $U_{11}^T (L_{11c}^T W_{11} L_{11c}) U_{11} = \Lambda_{11}^T$.
4. Formation of T_{11} : $T_{11} = L_c U_{11} \Lambda_{11}^{-1/2}$

The same procedure with appropriate subscript substitutions can be used to find T_{22} . Once both T_{11} and T_{22} are found, the overall transformation matrix T can be found by performing an operation denoted by \oplus in [21].

$$T = T_{11} \oplus T_{22} = \begin{bmatrix} T_{11} & \mathbf{0} \\ \mathbf{0} & T_{22} \end{bmatrix} \quad (14)$$

Using the balancing matrix T , a balanced realization of the system can be found by similarity transformation of state-space matrices as shown in Eq. 6-6.

$$\begin{aligned} \hat{A} &= T^{-1} A T \\ \hat{b} &= T^{-1} b \\ \hat{c} &= c T \\ \hat{d} &= d \end{aligned} \quad (15)$$

By observing how many significant Hankel singular values exist, one can make the decision on how many states should be preserved thereby determining the order r_1 and r_2 . The state-space matrices can then be partitioned using the following scheme.

$$\begin{aligned} \hat{A} &= \begin{bmatrix} \hat{A}_1 & A_2 \\ \hat{A}_3 & A_4 \end{bmatrix} = \begin{bmatrix} A_{1r} & * & A_{2r} & * \\ * & * & * & * \\ \mathbf{0} & \mathbf{0} & A_{4r} & * \\ \mathbf{0} & \mathbf{0} & * & * \end{bmatrix} \\ \hat{b} &= \begin{bmatrix} \hat{b}_1 \\ \hat{b}_2 \end{bmatrix} = \begin{bmatrix} b_{1r} \\ * \\ b_{2r} \\ * \end{bmatrix} \\ \hat{c} &= [c_1 \mid c_2] = [c_{1r} \quad * \mid c_{2r} \quad *] \end{aligned} \quad (16)$$

A_{1r} is a $[r_1 \times r_1]$ matrix if r_1 is greater than r_2 and a $r_1 \times r_2$ matrix if r_2 is greater than r_1 . On the other hand A_{2r} is a $r_2 \times r_1$ matrix if r_1 is greater than r_2 and a $[r_2 \times r_2]$ matrix if r_2 is greater than r_1 . The dimensions of A_{3r} and A_{4r} are the same of that of A_{1r} and A_{2r} , respectively. Finally, the reduced system is obtained by forming new system matrices by

$$\begin{aligned} A_r &= \begin{bmatrix} A_{1r} & A_{2r} \\ A_{3r} & A_{4r} \end{bmatrix} \\ b_r &= \begin{bmatrix} b_{1r} \\ b_{2r} \end{bmatrix} \\ c_r &= [c_{1r} \mid c_{2r}] \end{aligned} \quad (17)$$

The resulting system which is described by the matrices A_r , b_r , and c_r is of order of $[r_1 \times r_2]$. From the new 2-D state-space description of the reduced system, one can obtain the 2-D system transfer function of lower order.

3.4 Filter Order Reduction Using Balanced Approximation: An Example

In this section, a 15x15 order bandpass filter is designed using optimal decomposition method, and the balanced approximation method is applied to reduce the filter order.

Application of balanced approximation method for 2-D filter order reduction

Design Aim: 2-D bandpass filter with normalized passband frequency between 0.33 and 0.66 with lowest order acceptable.

Method Used: Optimal decomposition for filter design, and balanced approximation for order reduction.

Programs Used: ODFIR2-D.m, BA.m

Results: Using optimal decomposition method, a filter with specifications shown below is designed. The error is approximated at 11% after 6 stages of approximations.

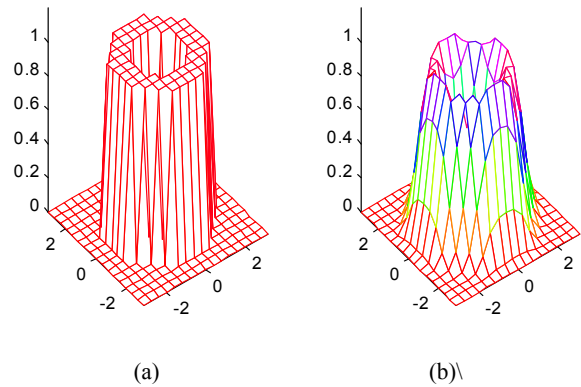


Figure 8: (a) Ideal magnitude response of the filter and (b) Actual filter response of the 16x16 order filter

Balanced approximation is then applied to the filter design. To apply the order reduction however, a new reduced order had to be chosen and the choice is made based on the Hankel singular values of the system plotted in Figure 9. Clearly, it seems reasonable to retain only up to 10th order

in both dimensions since from 11th order onwards, the Hankel singular values become very small indeed.

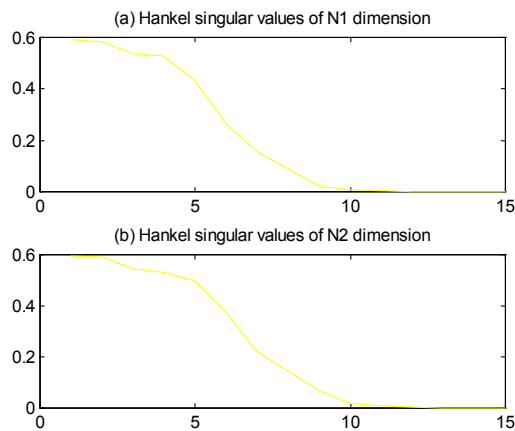


Figure 9: Hankel singular values of the filter

Choosing the new order of the filter as 10×10 , the BAM is applied with the following excellent results.

As the plots of magnitude characteristic shows, there is hardly any difference between the original design and the reduced order design. The error estimate of 11.46% compared to 11% of the original 15×15 order design confirms this point and shows that balanced approximation indeed produces filters of significantly lower order with very little sacrifice in performance.

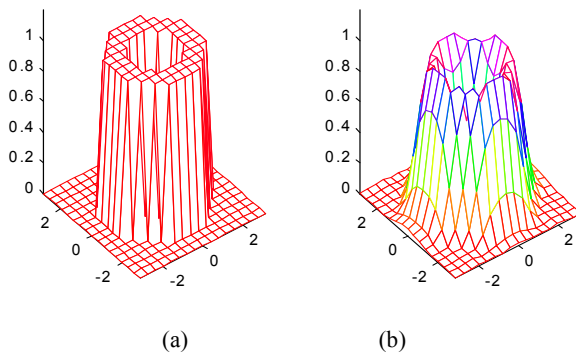


Figure 10: Reduced order (10×10) filter (a) Ideal characteristic of the filter (b) Actual characteristic of the filter

The result of application of BAM to a 2-D filter transfer function can be summarized as follows: (i) Reduced order filter; (ii) Usually IIR structure; (iii) If the original filter has a separable denominator, then the reduced filter also has a separable denominator allowing a separable implementation; and (iv) Little sacrifice in performance (magnitude error and phase linearity). The phase remains nearly linear for the resulting IIR structure

as well which is a feature difficult to achieve with other 2-D IIR filter design methods. The proof of the linearity is given in [5].

All in all, the BAM provides an excellent method of reducing filter order to a realizable level without a large deterioration in performance and should therefore be given a consideration before implementation of 2-D filters.

4. Fiber-Optic Delay Line Filters

As introduced in Part I [1], fiber optic delay line architecture is an alternative architecture to spatial and temporal architecture. The fiber optic delay line architecture used in this paper to implement 2-D filters is described in further detail with a mathematical analysis.

4.1 Coherent and Incoherent Operation of Photonic Filters

When the advances in laser technology first made guided wave photonic systems possible, most pioneering photonic systems used multi-mode propagation of light as the main mode of signal transmission. However with the advent of lasers with narrower line-widths, it has become possible to operate lightwave systems in single mode resulting in greater bandwidth-distance product. Single mode systems are becoming increasingly popular and the trend towards single mode systems is set to continue.

Aside from the mode of propagation, another factor that determines the characteristic of a lightwave system is whether system is operating in coherent or in incoherent modes. The differences between the two operations can be summarized as follows: in a coherent system, the light source can be regarded as operating in a single wavelength (although in reality, no matter how small the linewidth is, the emitted lightwave is certain to contain more than one wavelength component). The use of coherent light as the signal carrier simply means that the phase as well as the amplitude of the lightwaves must be regarded as a part of the information being carried by the lightwave. In incoherent systems, the information is carried only by the intensity of the lightwave. One may therefore consider incoherent systems as the amplitude modulated system with intensity modulation instead of amplitude modulation. It is obvious that negative range cannot be expressed by intensity-based incoherent systems unless one biases the light intensity to a predefined level. The receiver can then detect negative range by comparing the received intensity value to the predefined level.

The differences between coherent systems and incoherent systems are shown in Table 2. For signal processing purposes, incoherent operation implies that the modulating frequency of the source must be much lower than the

photonic frequency implying that the full bandwidth of the laser cannot be used. Coherent operation on the other hand allows utilization of the full bandwidth of the system resulting in greater processing speed. However, because coherent systems tend to be more vulnerable to environmental effects such as phase jitter, some shielding must be used to reduce the adverse effects to a negligible level [3]. Another important advantage coherent systems have over incoherent systems is the flexibility in system design. Incoherent systems fall into the category of so called *positive systems* and have restrictions on quantities such as number and positions of system poles and zeros [5]. In spite of such constraints, most of the research works reported so far on fiber-optic delay line signal processing have been using incoherent systems [3-7]. The reasons for avoiding coherent systems have been that ‘coherent systems are more difficult to implement in practice and are usually more complicated than incoherent systems because of the stringent requirements on the stability of the source and photonic delay paths’ [4]. In future however, it is likely that lasers capable of coherent operation over longer distances as well as better techniques for controlling the delay paths will be available. Coherent systems thus may yet represent the possibility for full bandwidth all-photonic processing.

	COHERENT SYSTEM	INCOHERENT SYSTEM
Information carrier	amplitude, phase	intensity
Bandwidth	very wide	wide
Required linewidth of the source	very narrow	narrow
Negative range	amplitude and phase can combine to express a negative value	predetermined bias value is necessary

Table 2: Differences between coherent and incoherent lightwave system

4.2 Using Optical Fibers to Realize Delayed Line Filter

Three main components are required in most forms of discrete-time filters: delay, coefficient, and summer/splitter. To illustrate how the components are realized in photonic domain, discrete-time tab filter shown in Figure 11 is used as an example. As the signal flow diagram for a discrete time tab filter is general, the photonic components used to realize a discrete-time tab-filter can be used in other filter structures.

4.2.1 Photonic Realization of Delay

In fiber-optic delay line filters, photonic fibers are used as delay elements as signal propagation time can be

controlled using the length of the fiber. The transfer function of optical fiber, ignoring the fiber signal dispersion and the fiber intensity loss, can be expressed mathematically by.

$$H(\omega) = e^{-j\beta L} \tag{18}$$

where L is the length of the delay lines, β is the propagation constant of the guided fundamental mode. The propagation constant β is defined by $\beta = \omega n_{eff}/c$ where n_{eff} is the effective refractive index of the guided mode in the fiber or optical planar channel waveguide, ω is the operating optical frequency in radians, and c is the speed of light. The inverse of the time delay T is $n_{eff}f/c$ and equals to the sampling frequency of the filter. Choosing a reference length of the optical delay as L_d , if L is a integer multiple of L_d the transfer function can be expressed as

$$H(\omega) = e^{-jd(L\frac{2\pi f n_{eff}}{c})} \dots\dots(a)$$

$$z^{-d} = e^{-jd(\omega T)} \dots\dots(b)$$

Upon comparing (19) (a) and (18) (b), it can be observed that the two equations are very similar and in fact, if ωT in (19)(b) is replaced by $(2\pi f)(n_{eff} L_d/c)$, then the two equations are identical. It is therefore clear that fiber can act as a delay whose length is controlled by n_{eff} and L .

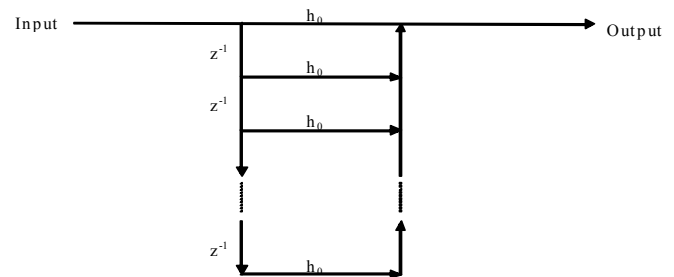


Figure 11: Signal flow diagram of discrete-time tab filter, the unit delay is the traveling time of lightwaves over a distance equivalent to the unit sampling time. The coefficients h 's are the transmittances over the specific path.

Optical fiber has several properties which enable it to be an ideal delay line medium: flexibility which enables a relatively compact implementation of the system, the accuracy of time interval between tabs that can be produced, insensitivity to electromagnetic interference which is useful when used in electro-magnetic environments - quite often the case with signal processing equipment.

4.2.2 Photonic Realization of Tap Coefficients

General form of a feed forward transfer function in z-domain can be expressed as.

$$H(z) = \sum_{d=0}^n h_d z^{-d} \tag{20}$$

There are several ways to realize the coefficients magnitude $|h_d|$ such as OAs /attenuators[6](earlier methods of achieving filter coefficients included reflectors, radiation due to bending, and evanescent coupling by polishing the cladding down very close to the fiber core [8]). However the negative sign can be difficult to realize as it represents a negative intensity in an incoherent system! The inability to represent negative quantities effectively is a major limitation of incoherent systems. On coherent systems a multiplication by a negative coefficient represents a phase shift of 180°.

4.2.3 Photonic Realization of Summer/Splitter

In photonic domain, summing/splitting of signals can be performed by optical couplers (see Figure 12).

$$\begin{bmatrix} E_3 \\ E_4 \end{bmatrix} = \begin{bmatrix} \sqrt{1-k_1} & -j\sqrt{k_1} \\ -j\sqrt{k_2} & \sqrt{1-k_2} \end{bmatrix} \begin{bmatrix} E_1 \\ E_2 \end{bmatrix} \tag{21}$$

Splitting of signal can be performed by using just one of the input terminals (E_1, E_2) and both output terminals (E_3, E_4) - see Figure 13(a). Summing can be achieved by using just one output signal port and both input ports - see Figure 13(b).

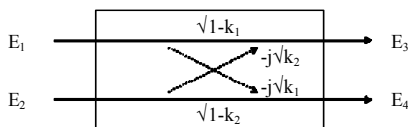


Figure 12: Schematic diagram of an optical coupler

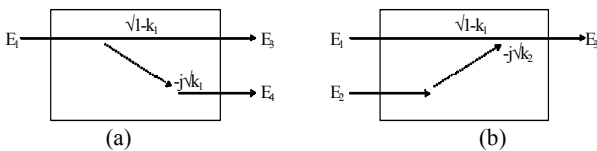


Figure 13:(a) Optical coupler as a splitter (b) Optical coupler as a summer.

When using an optical coupler as a summer/splitter, there are two undesirable properties that must be taken into account. Firstly, as can be seen from the transfer matrix, when photonic signal goes through a coupler the signal amplitude (and therefore intensity) is attenuated by the

coupling factor of the optical coupler which for a half intensity splitter is $1/\sqrt{2}$. A photonic filter is likely to have cascaded stages of optical couplers and the combined coupling coefficients cause quite substantial attenuation of the original input. OAs are therefore usually necessary to compensate for the amplitude attenuation [6]. Second problem arising from the use of optical couplers as splitter/summer is the phase shift of -90° associated with cross-coupling of photonic signals. The phase shift is not an issue for concern in an intensity-based system (incoherent system), however it can cause difficulty in coherent systems, especially when coupler is being used as a summer as the signals that are being added must be in the same phase at the output of the coupler. To illustrate this problem, consider adding two signals E_1 and E_2 that are in phase before they enter the coupler (21). At the output of the coupler, only one output is cross-coupled and therefore phase shifted whereas the other output retains the phase of the input signal. The added signal is therefore an inaccurate representation of the summing operation.

$$\begin{bmatrix} E_{out} \end{bmatrix} = \begin{bmatrix} \sqrt{1-k_1} & -j\sqrt{k_1} \\ -j\sqrt{k_2} & \sqrt{1-k_2} \end{bmatrix} \begin{bmatrix} E_1 \\ E_2 \end{bmatrix} \tag{22}$$

$$E_{out} = \sqrt{1-k_1}E_1 - j\sqrt{k_1}E_2$$

However, the phase shifting property of couplers, if manipulated well can act be used as perfect phase-shifters necessary in implementing negative coefficient taps. It is therefore conceivable that with the right choice of input and output terminals, a coherent signal processing system that represents negativity without biasing (as in incoherent systems) is feasible.

4.3 Graphical Representation of Photonic Circuits

A photonic circuit can be translated directly into a signal flow diagram (SFG) as the elements in an photonic circuit and the elements in its SFG have a direct one-to-one correspondence. To effectively utilize the SFG representation in analyzing photonic circuits, the well known Mason's rule² of analyzing the SFGs is applied to the photonic circuits [5]. The key to the application of the rule is the planar SFG representation of optical coupler as shown in Figure 14 [5].

Photonic components other than couplers such as fiber delay lines and amplifier/attenuators have a straightforward representation in the SFG. Using the above representation for optical couplers, photonic circuits can be analyzed systematically. The result is a very powerful technique that

² Mason's rule can be found in many digital signal processing textbooks. The rule is applied without modifications to SFG representations of optical circuits.

enables a systematic mathematical analysis of photonic lumped circuits. Using this technique, the z-transfer function of a system from any one node to another (instead of just from one preset input node to a preset output node) can be calculated allowing the system designer more degrees of freedom in designing and using photonic circuits. Once the transfer function in z-domain has been obtained, as z-transform theory is very well developed one can simply apply the conventional analysis to the photonic circuits.

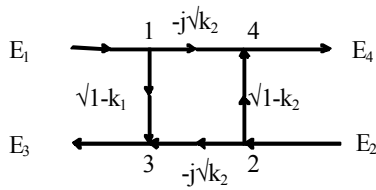


Figure 14: Graphical representation of optical coupler

Alternative to this method of analyzing photonic circuit is the matrix-method which attempts to analyze photonic circuit by direct manipulation of the coupler transfer matrix. The disadvantage of such approach is that when the photonic circuit consists of more than a few photonic elements, it becomes extremely difficult to recognize what effect each element is having on the overall function of the system. Graphical approach allows direct manipulation of the photonic circuit as the correlation between a SFG and the photonic circuit it represents is very high.

The graphical method is best suited to analyzing a lumped photonic system, most likely to confirm the operations of an photonic circuit or to find new functions of an photonic circuit configuration. For further discussion on the uses of the graphical method, see Part I [1].

Graphical method of analysis of double-coupler feedback photonic resonator

Double coupler feedback photonic resonator (DCFBOR) is a configuration which results in one optical energy storage element through feedback and one interferometer through different path lengths in the feed forward path. The resulting transfer function contains one pole and one zero at the origin, and therefore the configuration can be used to realize all pole IIR filters.

Method: Graphical technique for photonic circuit analysis [5]

Result: The photonic circuit of double coupler feedback optical resonator is shown in Figure 15. The SFG of DCFBOR is shown in Figure 16.

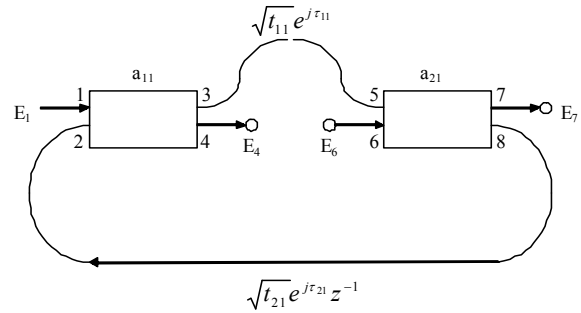


Figure 15: Schematic diagram of DCFBOR

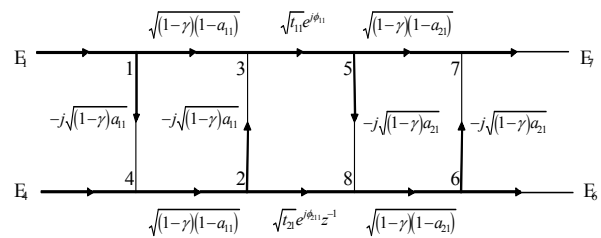


Figure 16: Signal flow diagram representation of DCFBOR

The details of application of Mason’s rule of determining the signal flow diagram transfer functions can be found in [5]. The resulting transfer function, as expected has one zero at the origin and one pole at a location in z-plane determined by the circuit parameters.

$$H(z) = \frac{E_7}{E_1} = \frac{(1-\gamma)\sqrt{(1-a_{11})(1-a_{21})}t_{11}e^{j\theta_{11}}}{1 + (1-\gamma)\sqrt{a_{11}a_{21}t_{11}t_{21}}e^{j(\theta_{11}+\theta_{21})}z^{-1}} \quad (23)$$

In conclusion, the graphical technique presents a previously unavailable systematic method of analysing photonic circuits. The greatest potential will be realized when the technique is implemented in a software form as the technique can be time-consuming to apply manually if there are more than two feedback loops.

4.4 Remarks

In this section we have described: (i) The differences between coherent and incoherent operation of lightwave systems. (ii) The architecture and components of delayed line filters; (iii) Table 3 showing components that make up a photonic digital filter with corresponding element in a SFG.

(iv) A method of representing photonic circuits in signal flow diagram is introduced and its advantages are outlined. It is stated that using Mason’s rule, the transfer function of an photonic circuit can be obtained directly

from signal flow diagrams. An example of application of the graphical method is also given.

Photonic implementation	Signal flow diagram element
unit length fiber	delay line
optical amplifier, optical attenuator, etc.	multiplicative coefficient
coupler	summing/splitting point

Table 3: Comparison of photonic and signal flow diagram elements.

5. Concluding Remarks: Part II

The objective of the research presented in this Part II paper is to explore possible ways of realizing a 2-D signal processing system using fiber-optic signal processing architecture. A general technique for designing a 2-D filter is illustrated and numerous examples of utilization of the technique are given. Although the discussion is focused on fiber-optic systems, the design procedure for 2-D filters are just as applicable to any other signal processing architectures. For example, the 2-D filter order reduction method given in *Section 3* can be used to simplify 2-D lightwaves systems which may or may not be fiber-optic systems.

The design of 2-D filters is classified into two different classes. One class used matrix decomposition to reduce the design of 2-D filters into a set of 1-D filter design procedures. The other class used direct extensions of 1-D filter design methods. It is found that neither has a distinctive superiority over another and that the designer has to choose what is the best for the particular application, most likely by designing both and comparing the performances. All of the design procedures are implemented using the MATLAB™ programming language.

Among the matrix decomposition methods, the multiple stage singular value decomposition method of *Section 3.2* performed the best whereas for direct methods, frequency sampling method produced filters with smallest errors. However, the result should be taken with caution as there are many factors to be considered before declaring one method superior over another. The differences between the various methods are outlined.

A 2-D Filter order reduction method is applied to make fiber- and integrated optic signal processing more feasible. The technology allows the filter designer to produce filters of orders that are implementable in practice without sacrifices in performance.

Different possible filter structures are proposed and illustrated for photonic implementation of 2-D filters. Most

of the filter structures discussed can be used in 1-D coherent fiber-optic signal processing and are not limited to 2-D coherent fiber-optic signal processing. Some of the proposed structures such as transversal structure are extremely efficient in the number of components used to achieve a certain performance requirement. To make the efficient structures possible, the phase shifting property of optical couplers when the incoming lightwaves is cross-coupled is utilized. Filter structures for FIR and IIR filters are also shown and examples are given in *Section 9*.

It is evident that the fiber-optic signal processing technology presents a new direction in the usage of optical fiber, lasers, and photonics technologies which are evolving very fast. In [4] an incoherent signal processing system operating at 100 MHz is demonstrated. The authors note that the raising this capability to over 10 GHz is a relatively straightforward procedure involving shorter fiber lengths and lasers and detectors with faster rise and fall time. They also note that although conventional digital signal processing and analog signal processing techniques are limited in their usefulness for signal bandwidths exceeding one or two GHz. Current research efforts on fiber-optic signal processing on lightwaves of millimeter wavelength region will allow signal processing at bandwidths of up to 100 GHz even to THz region if parametric amplification is employed. The field of 2-D signal processing which requires ultra-fast processing capability has a great deal to gain from the usage of the high speed processing capability of fiber-optic architectures. In particular especially with the fast pace of research and inventions of photonic circuits reaching the nano-scale employing photonic crystal wave guiding techniques will allow multi-dimensional processing in the photonic domain flourishing in the near future.

References

- [1] L.N. Binh, "Multi-dimensional Photonic Processing: A Discrete-Domain Approach", *Int. J. Computer Sc. And Network Security*, vol., 2009.
- [2] R. E. Twogood, S. K. Mitra, "Computer-aided design of separable two-dimensional digital filters," *IEEE Trans. Acoustic Speech. Signal Proc.*, Vol. ASSP-25, No. 2, April 1977, pp 165-169
- [3] T.B. Deng, M. Kawamata, and T. Higuchi, "Design of 2-D digital filters based on the optimal decomposition of magnitude specifications," *IEEE J. Circuits, Systems, and Computers*, Vol. 3, No. 3, 1993.
- [4] T Deng, M. Kawamata, "Frequency-Domain Design of 2-D digital filters using the iterative singular value decomposition," *IEEE Trans. Circ. Systems*, Vol. 38, No.10, Oct 1991, pp 1225-1228.
- [5] Le Nguyen Binh, "Photonic Signal Processing: Techniques and Applications", CRC Press Pub., Boca Raton, FL, USA, 2009.
- [6] T Deng, M. Kawamata, "Frequency-Domain Design of 2-D digital filters using the iterative singular value decomposition," *IEEE Trans. Circ. Systems*, Vol. 38, No.10, Oct 1991, pp 1225-1228.
- [7] A.K. Shaw and P. Mitra, "An exact realization of 2-D IIR filters using separable 1-D modules," *IEEE Trans. Circuits Syst.*, vol. 37, 1990.
- [8] F.T.S. Yu and I.C. Khoo, *Principles of Optical Engineering*, Section 9.



Le Nguyen Binh received the degrees of B.E. (Hons) and PhD in Electronic Engineering and Integrated Photonics in 1975 and 1980 respectively, both from the University of Western Australia, Nedlands, Western Australia. In 1981 he joined in the Department of Electrical Engineering of Monash University after a three year period with CSIRO Australia as

a research scientist developing parallel micro-computing systems. He was appointed to reader of Monash University in 1995. He has worked for and lead major research and development programs in the Department of Optical Communications of Siemens AG Central Research Laboratories in Munich and the Advanced Technology Centre of Nortel Networks in Harlow, U.K. He was a visiting professor in 2007-2008 and is currently an adjunct professor of the Faculty of Engineering of Christian Albrechts University of Kiel, Germany.

Dr. Binh has published more than 200 papers in leading journals and international conferences and three books, one on Photonic Signal Processing (2007) and the other on Digital Optical Communications (2008) both by the publishing house CRC Press (Florida, USA). His third book scheduled for publication in 2009 is "Optical Fiber Communications Systems: Principles, Practices and MATLAB Simulink Models" also by the same publisher. He is an associate editor of the International Journal of Optics and the Research Letters in Optics, Series Editor of the Series "Optics and Photonics" for CRC Press Pub.

His current research interests are Tb/s optical transmission systems and networks, especially advanced modulation formats and associate electronic equalization methods, photonic signal processing, integrated photonics and multi-bound soliton fiber lasers.